Acta Neurochir (2014) 156:2295–2302
DOI 10.1007/s00701-014-2236-0

CLINICAL ARTICLE - NEUROSURGICAL TECHNIQUES

Localizing hand motor area using resting-state fMRI: validated with direct cortical stimulation

Tian-ming Qiu · Chao-gan Yan · Wei-jun Tang · Jin-song Wu · Dong-xiao Zhuang · Cheng-jun Yao · Jun-feng Lu · Feng-ping Zhu · Ying Mao · Liang-fu Zhou

Received: 10 July 2014 / Accepted: 8 September 2014 / Published online: 24 September 2014

Abstract
Background Resting-state functional magnetic resonance imaging (R-fMRI) is a promising tool in clinical application, especially in presurgical mapping for neurosurgery. This study aimed to investigate the sensitivity and specificity of R-fMRI in the localization of hand motor area in patients with brain tumors validated by direct cortical stimulation (DCS). We also compared this technique to task-based blood oxygenation level-dependent (BOLD) fMRI (T-fMRI).
Methods R-fMRI and T-fMRI were acquired from 17 patients with brain tumors. The cortex sites of the hand motor area were recorded by DCS. Site-by-site comparisons between R-fMRI/T-fMRI and DCS were performed to calculate R-fMRI and T-fMRI sensitivity and specificity using DCS as a "gold standard". R-fMRI and T-fMRI performances were compared statistically
Results A total of 609 cortex sites were tested with DCS and compared with R-fMRI findings in 17 patients. For hand motor area localization, R-fMRI sensitivity and specificity were 90.91 and 89.41 %, respectively. Given that two subjects could not comply with T-fMRI, 520 DCS sites were compared with T-fMRI findings in 15 patients. The sensitivity and specificity of T-fMRI were 78.57 and 84.76 %, respectively. In the 15 patients who successfully underwent both R-fMRI and T-fMRI, there was no statistical difference in sensitivity or specificity between the two methods (p=0.3198 and p= 0.1431, respectively)
Conclusions R-fMRI sensitivity and specificity are high for localizing hand motor area and even equivalent or slightly higher compared with T-fMRI. Given its convenience for patients, R-fMRI is a promising substitute for T-fMRI for presurgical mapping

Keywords Resting-state fMRI · Effectiveness · Task-based BOLD fMRI · Direct cortical stimulation · Hand motor area

Tian-ming Qiu and Chao-gan Yan contributed equally to this paper.

T.-m. Qiu · J.-f. Lu · F.-p. Zhu · Y. Mao · L.-f. Zhou (✉)
Neurological Surgery Department, Huashan Hospital, Shanghai Medical College, Fudan University, 12#, Wulumuqi Zhong Road, Shanghai 200040, People's Republic of China
e-mail: lfzhouc@126.com

C.-g. Yan
The Nathan Kline Institute for Psychiatric Research, Orangeburg, NY 10962, USA

C.-g. Yan
The Phyllis Green and Randolph Cowen Institute for Pediatric Neuroscience, New York University Child Study Center, New York, NY 10016, USA

W.-j. Tang
Department of Radiology, Huashan Hospital, Fudan University, Shanghai 200040, China

J.-s. Wu · D.-x. Zhuang · C.-j. Yao
Glioma Surgery Division, Neurological Surgery Department, Huashan Hospital, Shanghai Medical College, Fudan University, Shanghai 200040, China

Introduction

The accurate preoperative localization of motor areas can help optimize tumor resection and minimize morbidity and mortality [21, 28, 32]. Blood oxygenation level-dependent (BOLD) functional magnetic resonance imaging (fMRI) has been successfully adopted for noninvasively localizing eloquent areas before neurological surgeries. However, this conventional approach has prominent limitations. Patients suffering from paralysis or attention disorders are unable to cooperate adequately with the task-based paradigms. Head movements due to tasks may disturb the fMRI data analysis process. Preoperative localization and evaluation, which is time-consuming and labor-intensive, depends much on each patient's ability to accomplish the required tasks [19, 23].

Resting-state fMRI (R-fMRI) requires no tasks or external stimuli. Spontaneous BOLD fluctuations are used to present the functional networks. Also, a strong correlation is reproducibly present within sensorimotor networks [1, 6, 33]. After a seed was placed in the motor area on one side, spontaneous synchronous fluctuations throughout the brain, referred to as "functional connectivity," revealed the contralateral motor area [8, 9].

These findings made it possible for R-fMRI to be applied to identify the hand motor area. Several studies [13, 14, 24, 38] reported the preliminary application of R-fMRI for presurgical planning, but the sensitivity and specificity of this method compared with direct cortical stimulation (DCS), the "gold standard", are still missing. Therefore, this study aimed to determine whether R-fMRI is sufficiently sensitive or specific for hand motor area localization with DCS validation and investigate whether R-fMRI can be used as a substitute for conventional task-based BOLD fMRI (T-fMRI) in patients with brain tumors.

Methods

Subjects

Between March 2012 and January 2013, 17 patients (11 men and six women) with suspected cerebral gliomas adjacent to the motor area were enrolled in the study. Eligible patients were 23–67 years of age with a diagnosis of single, unilateral, supratentorial primary glioma. No contraindications for magnetic resonance imaging (MRI) were present. The exclusion criteria were as follows: secondary or recurrent gliomas, contraindications for MRI, and patients for whom initial muscle strength grade of the affected extremities was 0/5 (no contraction at all). For histopathological diagnoses, the World Health Organization classification of tumors of the nervous system (2007) was used. All protocols were approved by the Huashan Committee on Human Research at Fudan University, and written informed consent was obtained from each subject.

MRI data acquisition

All images were acquired on a Siemens Magnetom Verio 3.0 T MRI scanner (Siemens Medical Solutions, Erlangen, Germany). The patients were scanned preoperatively using R-fMRI (TR, 2,000 ms; TE, 35 ms; flip angle, 90°; slice number, 33; field of view [FOV], 240×240 mm; voxel size, 3.3×3.3×4.0 mm^3). Scans lasted for 8 min for a total of 240 time points per subject. During the scanning, subjects remained still with their eyes closed but did not fall asleep and were given no tasks. Each run was preceded by 6-s dummy scans to stabilize the magnets.

The T-fMRI data acquisition, which lasted for 3 min, consisted of trail blocks of finger tapping with 1-Hz frequency and rest blocks without given tasks. The task and rest blocks were repeated three times for each patient, and each block lasted 30 s. MRI data were acquired using a single-shot echo-planar imaging (EPI) sequence (TR, 3,000 ms; TE, 30 ms; flip angle, 90°; slice number, 46; FOV, 240×240 mm; voxel size, 2.5×2.5×3 mm^3). Each run was preceded by 8-s dummy scans to stabilize the magnets.

For those gliomas that could be enhanced, structural images were acquired using an axle magnetization-prepared rapid gradient echo T1-weighted sequence with contrasts (gadopentetate dimeglumine) (TR, 1,900 ms; TE, 2.93 ms; flip angle, 90°; matrix size, 256×215; slice number, 176; slice thickness, 1 mm; FOV, 250×219 mm). For gliomas without enhancement, structural images were acquired using an axle T2-weighted fluid-attenuated inversion recovery sequence (TR, 9,000 ms; TE, 99 ms; TI, 2,500 ms; flip angle, 150°; matrix size, 256×160; slice number, 66; slice thickness, 2 mm; FOV, 240×214 mm).

Preprocessing of imaging data

All imaging data were preprocessed using Statistical Parametric Mapping 8 (SPM8; Wellcome Department of Imaging Neuroscience, University College London, UK), Data Processing Assistant for Resting-State fMRI advanced edition (DPARSFA) [5] and Resting-State fMRI Data Analysis Toolkit (REST) [26]. R-fMRI data preprocessing was conducted at the individual level as follows. After the first ten time points were excluded, the images were corrected for slice timing and realigned. Each subject's structural image was co-registered to his/her mean EPI image to identify the anatomic localization of the functional foci. These images were smoothed using a Gaussian kernel with full-width at the half maximum of 4 mm. The linear trend over each run was removed and then a temporal band-pass filter (0.01 Hz$<$f$<$0.08 Hz) was applied to the times. The spurious BOLD variances that were unlikely to reflect neuronal activity were regressed out [7, 9]: the parameters obtained by rigid body head motion correction, the signals from white matter and cerebrospinal fluids, as well as global mean signal.

Task activation

For the T-fMRI data, slice timing correction was not performed because it was a blocked design and the time shift was quite small compared with the block length [18]. We corrected the volumes for head motion and co-registered the EPI images to those structural images that have been co-registered to his/her R-fMRI images. The images were smoothed with a Gaussian kernel of 4 mm. These task data were analyzed using the general linear model in SPM8 to

identify the region of the brain that correlated with finger tapping. The top 2 % of the highly activated voxels for each case was extracted for visualization (Xjview8, http://www.alivelearn.net/xjview) and statistical analysis.

Seed-based functional connectivity

The seed region localized to the motor area was selected at the hand-knob area [4] of the healthy hemisphere. This area is easily distinguished on high-resolution structural MRI films and has been confirmed to be a reliable landmark for identifying the precentral gyrus under normal or even pathological conditions [35]. After identifying the hand-knob area, a spherical region of interest (ROI) with a radius of 3 mm was seeded there for functional connectivity analysis. The mean time course in the ROI was then extracted and its correlation with every other voxel in the brain was calculated. After all voxels were sorted by correlation coefficient, the top 2 % of the highly correlated voxels for each case was extracted for visualization and statistical analysis.

Direct cortical stimulation

The fMRI was validated by DCS in 17 patients. Using a Multifunctional Neurological Workstation (Epoch XP; AXON, NY, USA), a biphasic square-wave pulse at 60 Hz was delivered through a 5-mm-wide bipolar electrode per square centimeter. The current amplitude was progressively increased by 1 mA (range, 2–6 mA). The after-discharge activity was recorded using a six-contact strip subdural electrode during the progress of DCS. If after-discharge activity was captured, indicating that the stimulation current was too high, the current amplitude was decreased by 0.5–1 mA. Compound muscle action potentials (cMAPs) at abductor pollicis brevis, brachioradialis, triceps brachii, biceps brachii, tibial muscle, gastrocnemius, and orbicularis oris were recorded during DCS. The cortical motor sites were identified when the cMAPs (abductor pollicis brevis, brachioradialis, triceps brachii, or biceps brachii for the hand; tibial muscle or gastrocnemius for the leg; orbicularis oris for the mouth) were recorded when passive movements of the target muscle were found. Sterile tags were then used to mark the cortical sites on the surface of the cortex. Positive sites were then recorded by snapshot photography using a neuronavigation system (TRIA i7; Medtronic Navigation, Minneapolis, MN, USA).

Statistical analysis

Site-by-site comparisons between R-fMRI/T-fMRI and DCS were performed as follows. DCS results and fMRI data were considered to match if they were within the same 1-cm range. We recorded the anatomical position of each recorded DCS positive site on the three-dimensional functional MR image and overlaid a sphere with a 1-cm radius on each tag. For each case, the numbers of true-positive (TP), true-negative (TN), false-positive (FP), and false-negative (FN) tags were calculated. Each cortical site on the DCS map was considered independent. A similar method was used for the statistical analysis in earlier studies [2, 22]. A method for analyzing clustered binary data was used to calculate the sensitivity and specificity for R-fMRI/T-fMRI [10]. The Z test was used to compare the differences in sensitivity and specificity between these two methods.

Results

The patient characteristics are shown in Table 1. All patients had gliomas, including five with high grade and 12 with low grade. R-fMRI data were acquired for all 17 patients, while T-fMRI data were acquired for 15 since two could not cooperate well with the given task. DCS was performed for each of the 17 patients (Table 2). The interval between fMRI acquisition and DCS was <3 days.

A total of 609 DCS sites were tested and evaluated with the findings of the R-fMRI in 17 patients. For hand motor function, the overall sensitivity and specificity values of R-fMRI

Table 1 Patient characteristics

No.	Age	Sex	Location	Pathology	WHO glioma grade[a]
1	M	41	Left frontal	Astrocytoma	II
2	M	23	Left frontal	Astrocytoma	II
3	M	38	Left frontal	Astrocytoma	II
4	M	27	Left parietal	Oligoastrocytoma	II
5	F	51	Left frontal	Astrocytoma	II
6	F	36	Left frontal	Astrocytoma	II
7	F	67	Left frontal	Glioblastoma multiforme	IV
8	M	49	right parietal	Oligoastrocytoma	II
9	M	39	Left frontal	Astrocytoma	II
10	M	40	Left frontal	Glioblastoma multiforme	IV
11	M	49	Left frontal	Anaplastic astrocytoma	III
12	F	45	right frontal	Oligoastrocytoma	II
13	M	32	Left frontal	Astrocytoma	II
14	F	39	right frontal	Astrocytoma	II
15	M	50	Left frontal	Anaplastic astrocytoma	III
16	M	23	Left frontal	Astrocytoma	II
17	F	34	Left frontal	Astrocytoma	II

F female, *M* male, *WHO* World Health Organization

[a] According to the 2007 WHO classification of tumors of the central nervous system

Table 2 Correlation between functional MRI and DCS

	T-fMRI				R-fMRI			
No.	No. of TPs	No. of TNs	No. of FPs	No. of FNs	No. of TPs	No. of TNs	No. of FPs	No. of FNs
1	2	24	4	0	2	26	2	0
2	2	37	2	0	2	36	3	0
3	2	33	4	0	3	33	3	0
4	1	39	8	0	1	41	6	0
5	2	8	4	0	2	8	4	0
6	1	25	8	0	1	26	7	0
7	2	6	4	0	0	9	1	2
8[a]	/	/	/	/	1	32	2	0
9	1	33	6	0	1	38	1	0
10	2	34	2	1	3	34	2	0
11	1	40	3	2	2	36	7	1
12	0	35	7	1	1	36	6	0
13[a]	/	/	/	/	4	48	2	0
14	2	28	2	0	2	24	6	0
15	2	18	9	0	2	26	1	0
16	1	36	9	0	1	37	8	0
17	1	23	2	1	2	25	0	0

TPs true positives, *TNs* true negatives, *FPs* false positives, *FNs* false negatives, *T-fMRI* task-based functional magnetic resonance imaging, *R-fMRI* resting-state functional magnetic resonance imaging

[a] Patients failed to undergo the task-based paradigm

were 90.91 and 89.41 %, respectively. A total of 520 DCS sites were evaluated with the findings of the T-fMRI in the 15 patients. The sensitivity and specificity values for the hand motor area were 78.57 and 84.76 %, respectively. For these 15 patients who underwent both R-fMRI and T-fMRI, there was no statistical difference in sensitivity or specificity between these two methods (p=0.3198 and p=0.1431, respectively).

Illustrative cases

Patient 1

A 23-year-old man presented with a 1-month history of repeated headache. Preoperative MRI revealed a lesion located in the left frontal lobe, with proximity to rolandic area. He was scanned preoperatively using both T-fMRI and R-fMRI. T-fMRI revealed a pattern of activity in both hemispheres. A functional connectivity map was generated to localize the left hand area after seeding the hand-knob area on the contralateral hemisphere (Fig. 1a and b). One cortical site of the hand motor area was identified by DCS (Fig. 1c). Comparison of T-fMRI with DCS resulted in one TP, 36 TN and nine FP tags (Fig. 1e). Comparison of R-fMRI with DCS resulted in one TP, 37 TN and eight FP tags (Fig. 1f).

Patient 2

A 32-year-old man with a 1-month history of repeated seizure attacks was diagnosed with low-grade glioma in the left frontal lobe. Since he was unable to cooperate well with the task due to a mental disorder and could not undergo T-fMRI, he was scanned preoperatively with R-fMRI only. After an ROI in the normal right hand-knob area was seeded (Fig. 2a and b), a functional connectivity map was generated. Four cortical sites of the hand motor area were identified by DCS (Fig. 2c). Comparison of R-fMRI with DCS resulted in four TP, 48 TN and two FP tags (Fig. 2d).

Discussion

For patients with brain tumors, both brain anatomy and localization of the brain functional areas was distorted due to the lesions. It is of great importance to investigate the individual relationship between motor area and tumors. Hand function is most important in all motor functions, which largely affects patient quality of life after surgery. Most presurgical T-fMRI focused on showing hand motor areas [11, 32]. Thus, this study discussed hand motor localization using presurgical T-fMRI and R-fMRI. Although DCS is the current clinical gold standard for motor mapping [12, 16], it requires abundant

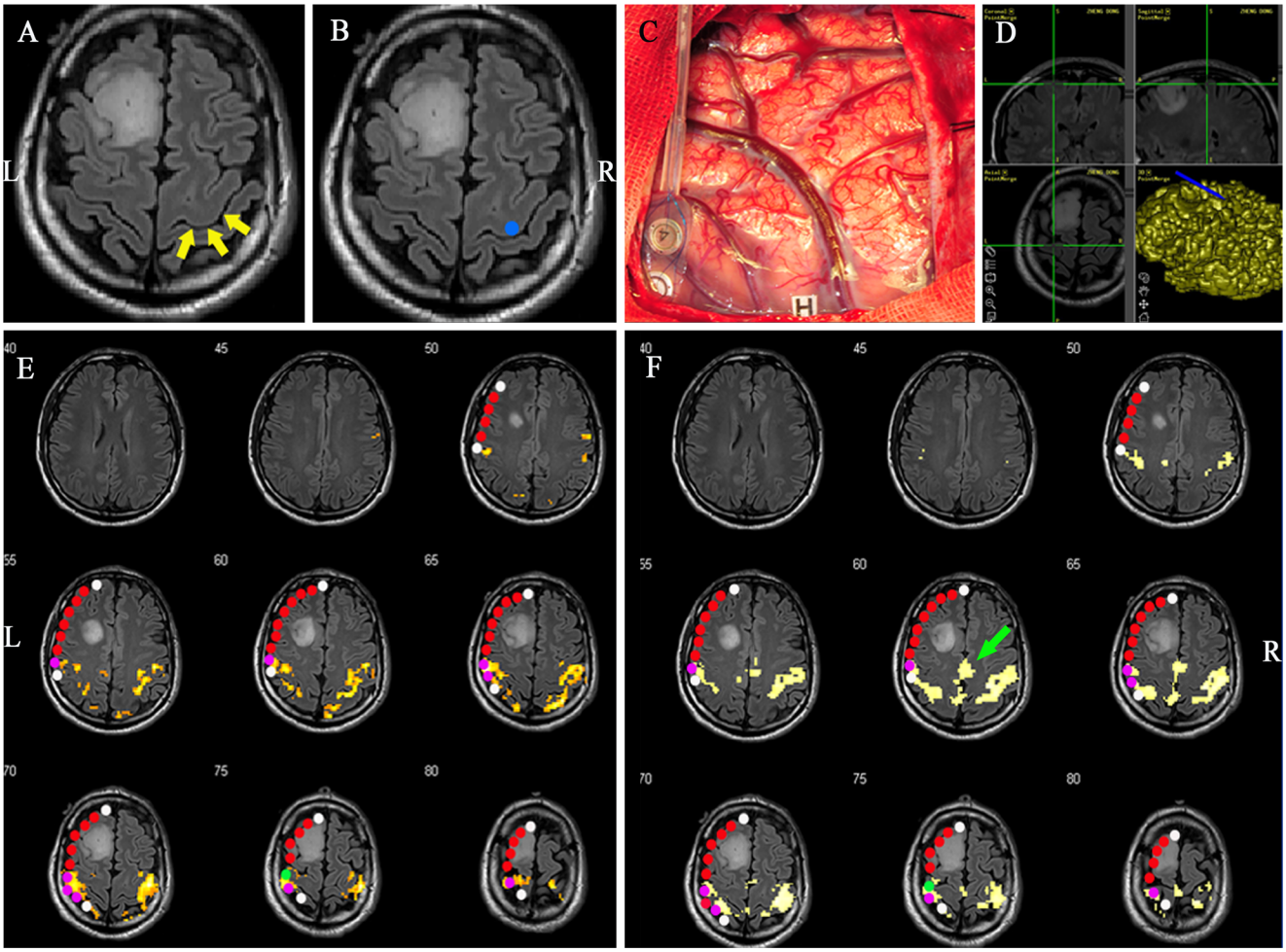

Fig. 1 Functional MRI and direct cortical stimulation mapping for case 16. Preoperative MRI revealed a lesion located in the left frontal lobe with proximity to the rolandic area. The *yellow arrows* show the right-side hand-knob area (**a**) where a region of interest (*blue circle*) (**b**) was seeded to generate a functional connectivity map. Of all of the 1-cm^2 sites within the bone window, one positive site for the hand motor area (tag *H*) was found by direct cortical stimulation (**c**) and then a snapshot taken via the neuronavigation system (**d**). Comparison of task-based blood oxygenation level-dependent with direct cortical stimulation resulted in 1 true-positive tag (*green*), 36 true-negative tags (*red*) and 9 false-positive tags (*pink*) within the bone window (*white*) (**e**). Comparison of resting-state fMRI with direct cortical stimulation resulted in 1 true-positive tag (*green*), 37 true-negative tags (*red*) and 8 false-positive tags (*pink*) within the bone window (*white*) (**f**). The *green arrow* shows the supplementary motor area on the R-fMRI map

experience of surgeons and additional time. As an invasive and intraoperative approach, it may also carry the risk of after-discharges which can induce seizures during operation [3, 30]. Preoperative evaluation by fMRI showed its clinical advantage over DCS.

Traditional T-fMRI has several limitations, and the ability of R-fMRI to overcome such limitations shows promise. In recent studies of motor area localization using R-fMRI, different methods were adopted on discrete cases. Zhang et al. [38] used functional connectivity to map the sensorimotor area. They confirmed the reproducibility of resting-state maps. In two cases, they found that R-fMRI maps were consistent with DCS maps. Resting-state independent component analyses can also be utilized to localize the sensorimotor area individually [13]. Liu et al. [14] found that presurgical motor mapping using R-fMRI showed similar results to those of T-fMRI in six cases. They also validated the functional mapping based on R-fMRI using DCS in one case. However, among all of these studies, R-fMRI was validated with DCS in only three cases. No papers provided the statistical results of the sensitivity and specificity of R-fMRI in presurgical motor mapping or whether it is equivalent to or better than T-fMRI. Thus, the purpose of this study is to determine whether R-fMRI is reliable compared with the gold standard of DCS in hand motor area localization and to investigate whether this method is comparable to conventional T-fMRI in patients with brain tumors.

In our study, the sensitivity and specificity for mapping hand motor area using R-fMRI was each around 90 %, which were both higher than those obtained with T-fMRI. However, there is no statistical difference in sensitivity or specificity between these two methods. R-fMRI proved to be reliable in

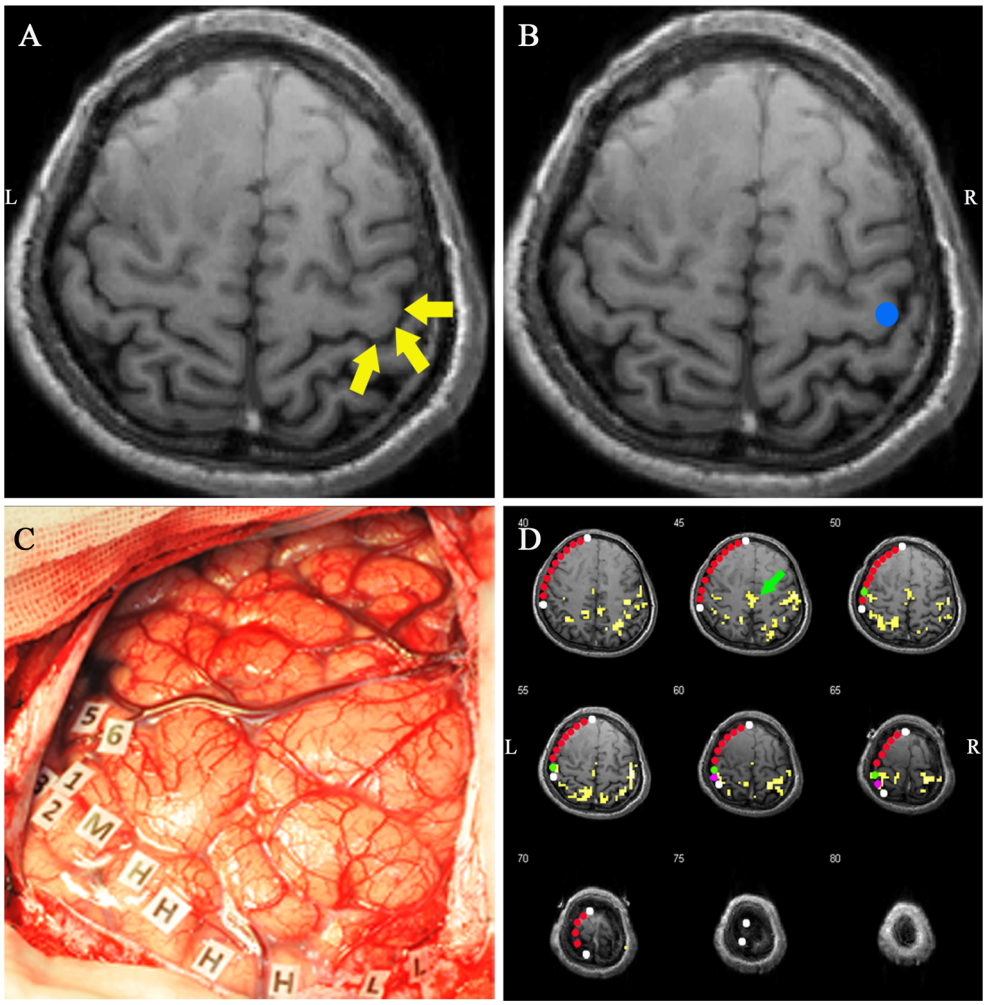

Fig. 2 Functional MRI and direct cortical stimulation mapping for case 13. Preoperative MRI revealed a lesion located in the left frontal lobe. *Yellow arrows* show the right-side hand-knob area (**a**) where a region of interest was seeded to generate a functional connectivity map (*blue circle*) (**b**). Of all of the 1-cm^2 sites within the bone window, four positive sites for the hand motor area (tag *H*), one site for the mouth area (tag *M*), two sites for the leg area (tag *L*), and five sites for the language area (tags *1*, *2*, *3*, *5*, and *6*) were found by direct cortical stimulation (**c**) and then a snapshot taken via the neuronavigation system. Comparison of resting-state fMRI with direct cortical stimulation resulted in 4 true-positive tags (*green*), 48 true-negative tags (*red*), and 2 false-positive tags (*pink*) within the bone window (*white*) (**d**). The *green arrow* shows the supplementary motor area on the R-fMRI map

hand motor area localization even when the patient failed to accomplish the task-based paradigm. These findings demonstrate the utility and validity of R-fMRI as a tool for preoperative hand motor localization. To some extent, the conventional T-fMRI can be substituted by R-fMRI.

R-fMRI was usually analyzed on the group level because these data should be processed by statistical methods. Most of the utilities were clinically focused on those brain diseases without obvious structural changes such as mental disorder [31, 36], metabolic encephalopathy [27, 39], primary epilepsy [17, 37], or neurodegeneration [29]. Although functional connectivity can be used to map the sensorimotor area on individual level, it is still difficult to unify the processing method for each case and, furthermore, evaluate its validity. One problem with seed-based functional connectivity analysis is where to put the seed region. The hand motor area can be easily identified as the knob-like structure in the precentral gyrus [4, 35], so we set the seed region on the hand-knob in the healthy hemisphere. Seed regions were set individually; therefore, normalization was unnecessary when preprocessing the data, which can be difficult when the tumor-induced distortion is present. Thus, its clinical use was more convenient. Tumors may induce plastic changes in the localization of motor areas [15, 34], and even lead to similar variations in the contralateral side [25]. In those cases in which R-fMRI didn't show satisfactory results, plasticity of motor areas might happen and lead to inaccuracies of seeding. For most cases in this study, the whole sensorimotor areas including supplementary motor area (Figs. 1f and 2d) were shown after putting seed region at contralateral hand-knob area, and the results were validated by DCS. The second problem is how to set the number of the correlated voxels after functional connectivity and unify all of the cases. In earlier studies, different *p* values were set as the threshold when viewing the result after functional connectivity in different cases. It was impossible to calculate the sensitivity and specificity for the case series or give any reliable information for data processing in another case. We extracted the top 2 % of the highly correlated voxels for R-fMRI and the top 2 % of the highly activated voxels for T-fMRI. All of the statistical analyses included the unified processed data. The third problem is how to calculate the sensitivity and specificity. We stimulated all sites in the

bone window and marked positive DCS sites on the navigated MRI images, then obtained the TP, TN, FP, and FN sites. The sensitivity and specificity of both R-fMRI and T-fMRI can be calculated and compared statistically.

Even though the validity of R-fMRI in preoperative motor mapping was confirmed in this study, there are still some limitations of R-fMRI in presurgical planning and further clinical use. First, R-fMRI data processing requires time and experience. The seed region must be set manually, which makes data processing difficult to automate. Seeding the hand-knob area makes it possible to process the data in the individual space; therefore, we expedited the process by omitting the normalization steps to the standard space and masking out the tumor. For process speed and efficiency, therefore, more automated analysis software and image creation will be required. Second, this method is not fully suitable for language mapping using R-fMRI due to the difficulty in seeding the language network, which is known to be unilateral and more variable across patients. In our earlier study, we tried to place a priori a seed region on the mirror site opposite Broca's area to obtain the language map, but the sensitivity of R-fMRI in revealing language area was only 47.8 % [20]. As such, this method can play only an ancillary role in the localization of the language area. However, we recently successfully created a Chinese language template using DCS in another study (submitted), which may help seed the language network. Third, R-fMRI data must be converted to a NIFTI file when processed, which is unacceptable in most current navigation systems. Therefore, these images cannot be used in a neuronavigation system. Recently, some software that enables the conversion of NIFTI files back to DICOM files is available online (http://www.bio.dist.unige.it/), which may make it possible to navigate using R-fMRI in surgeries. However, these results from processed R-fMRI data can provide presurgical information but not a real-time evaluation due to brain shifting after the tumor removal. In the future, intraoperative MRI scan can be very important for neurosurgeons making intraoperative decisions. Combined structural and functional images may be obtained from high-field intraoperative MRI scans, which can help neurosurgeons evaluate the relationship between a shifted eloquent area and residual tumor during surgery and decide whether further resection is safe. Further studies would focus on the benefit of the use of R-fMRI for motor outcomes as well as overall survival after brain tumor surgery.

DCS is still the gold standard of cortical or subcortical motor mapping, and it cannot be substituted by fMRI. R-fMRI is a supplementary, but compromising tool in localizing motor cortex, especially beneficial for those cases in which DCS is not reliable or for patients who do not cooperate well with T-fMRI.

Conclusion

In the current study, we evaluated the validity of R-fMRI for localizing the hand motor area during presurgical planning. R-fMRI features high sensitivity and specificity and is a promising substitute for T-fMRI.

The authors would like to thank Jian-bing Shi and Zhong Yang for assembling the image database, Gen Xu for direct cortical stimulation, and Yan-yan Song for statistical analysis.

Author contributions Study concept and design: Zhou and Wu. Processing of data: Qiu, Zhuang, Yao, Lu, Zhu, and Tang. Analysis and interpretation of data: Qiu and Yan. Drafting of the manuscript: Qiu and Yan. Critical revision of the manuscript for important intellectual content: Wu, Mao and Zhou.

Financial Disclosure None reported.

Funding This work was funded by the National Natural Science Foundation of China (Project No. 81271517, 81171295), The National Key Technology R&D Program of China (No. 2014BAI04B05), and Shanghai Municipal Health Bureau (XBR2011022).

Conflict of interest None.

References

1. Biswal B, Yetkin FZ, Haughton VM, Hyde JS (1995) Functional connectivity in the motor cortex of resting human brain using echo-planar MRI. Magn Reson Med 34:537–541
2. Bizzi A, Blasi V, Falini A, Ferroli P, Cadioli M, Danesi U, Aquino D, Marras C, Caldiroli D, Broggi G (2008) Presurgical functional MR imaging of language and motor functions: validation with intraoperative electrocortical mapping. Radiology 248:579–589
3. Blume WT, Jones DC, Pathak P (2004) Properties of after-discharges from cortical electrical stimulation in focal epilepsies. Clin Neurophysiol 115:982–989
4. Boroojerdi B, Foltys H, Krings T, Spetzger U, Thron A, Topper R (1999) Localization of the motor hand area using transcranial magnetic stimulation and functional magnetic resonance imaging. Clin Neurophysiol 110:699–704
5. Chao-Gan Y, Yu-Feng Z (2010) DPARSF: a MATLAB Toolbox for "Pipeline" data analysis of resting-state fMRI. Front Syst Neurosci 4: 13
6. De Luca M, Smith S, De Stefano N, Federico A, Matthews PM (2005) Blood oxygenation level dependent contrast resting state networks are relevant to functional activity in the neocortical sensorimotor system. Exp Brain Res 167:587–594
7. Fair DA, Schlaggar BL, Cohen AL, Miezin FM, Dosenbach NU, Wenger KK, Fox MD, Snyder AZ, Raichle ME, Petersen SE (2007) A method for using blocked and event-related fMRI data to study "resting state" functional connectivity. Neuroimage 35:396–405
8. Fox MD, Corbetta M, Snyder AZ, Vincent JL, Raichle ME (2006) Spontaneous neuronal activity distinguishes human dorsal and ventral attention systems. Proc Natl Acad Sci USA 103:10046–10051
9. Fox MD, Raichle ME (2007) Spontaneous fluctuations in brain activity observed with functional magnetic resonance imaging. Nat Rev Neurosci 8:700–711

10. Jeong B, Choi J, Kim JW (2012) MRI study on the functional and spatial consistency of resting state-related independent components of the brain network. Korean J Radiol 13:265–274
11. Kim MJ, Holodny AI, Hou BL, Peck KK, Moskowitz CS, Bogomolny DL, Gutin PH (2005) The effect of prior surgery on blood oxygen level-dependent functional MR imaging in the preoperative assessment of brain tumors. AJNR Am J Neuroradiol 26: 1980–1985
12. Kim SS, McCutcheon IE, Suki D, Weinberg JS, Sawaya R, Lang FF, Ferson D, Heimberger AB, DeMonte F, Prabhu SS (2009) Awake craniotomy for brain tumors near eloquent cortex: correlation of intraoperative cortical mapping with neurological outcomes in 309 consecutive patients. Neurosurgery 64:836–845, discussion 345–836
13. Kokkonen SM, Nikkinen J, Remes J, Kantola J, Starck T, Haapea M, Tuominen J, Tervonen O, Kiviniemi V (2009) Preoperative localization of the sensorimotor area using independent component analysis of resting-state fMRI. Magn Reson Imaging 27:733–740
14. Liu H, Buckner RL, Talukdar T, Tanaka N, Madsen JR, Stufflebeam SM (2009) Task-free presurgical mapping using functional magnetic resonance imaging intrinsic activity. J Neurosurg 111:746–754
15. Mathews S, Oommen KJ, Francel P (2001) Functional reorganization of motor cortex due to brain tumor: a case report. J Okla State Med Assoc 94:7–11
16. Matz PG, Cobbs C, Berger MS (1999) Intraoperative cortical mapping as a guide to the surgical resection of gliomas. J Neurooncol 42: 233–245
17. Morgan VL, Sonmezturk HH, Gore JC, Abou-Khalil B (2012) Lateralization of temporal lobe epilepsy using resting functional magnetic resonance imaging connectivity of hippocampal networks. Epilepsia 53:1628–1635
18. Pekar JJ (2006) A brief introduction to functional MRI. IEEE Eng Med Biol Mag 25:24–26
19. Pujol J, Conesa G, Deus J, Lopez-Obarrio L, Isamat F, Capdevila A (1998) Clinical application of functional magnetic resonance imaging in presurgical identification of the central sulcus. J Neurosurg 88: 863–869
20. Qiu TM, Wu JS, Zhuang DX, Yao C, Lu J, Zhang J, Gong X, Mao Y, Zhou L (2012) Preliminary application of resting-state functional magnetic resonance imaging in localizing language cortex for glioma patients. Chin J Neurosurg 28:1196–1200
21. Roessler K, Donat M, Lanzenberger R, Novak K, Geissler A, Gartus A, Tahamtan AR, Milakara D, Czech T, Barth M, Knosp E, Beisteiner R (2005) Evaluation of preoperative high magnetic field motor functional MRI (3 Tesla) in glioma patients by navigated electrocortical stimulation and postoperative outcome. J Neurol Neurosurg Psychiatry 76:1152–1157
22. Roux FE, Boulanouar K, Lotterie JA, Mejdoubi M, LeSage JP, Berry I (2003) Language functional magnetic resonance imaging in preoperative assessment of language areas: correlation with direct cortical stimulation. Neurosurgery 52:1335–1345, discussion 1345–1337
23. Rutten GJ, Ramsey NF (2010) The role of functional magnetic resonance imaging in brain surgery. Neurosurg Focus 28:E4
24. Shimony JS, Zhang D, Johnston JM, Fox MD, Roy A, Leuthardt EC (2009) Resting-state spontaneous fluctuations in brain activity: a new paradigm for presurgical planning using fMRI. Acad Radiol 16:578–583
25. Shinoura N, Suzuki Y, Yamada R, Kodama T, Takahashi M, Yagi K (2006) Restored activation of primary motor area from motor reorganization and improved motor function after brain tumor resection. AJNR Am J Neuroradiol 27:1275–1282
26. Song XW, Dong ZY, Long XY, Li SF, Zuo XN, Zhu CZ, He Y, Yan CG, Zang YF (2011) REST: a toolkit for resting-state functional magnetic resonance imaging data processing. PLoS One 6:e25031
27. Spagnolli F, Cerini R, Cardobi N, Barillari M, Manganotti P, Storti S, Mucelli RP (2013) Brain modifications after acute alcohol consumption analyzed by resting state fMRI. Magn Reson Imaging 31:1325-1330
28. Talacchi A, Turazzi S, Locatelli F, Sala F, Beltramello A, Alessandrini F, Manganotti P, Lanteri P, Gambin R, Ganau M, Tramontano V, Santini B, Gerosa M (2010) Surgical treatment of high-grade gliomas in motor areas. The impact of different supportive technologies: a 171-patient series. J Neurooncol 100:417–426
29. Thomas JB, Brier MR, Snyder AZ, Vaida FF, Ances BM (2013) Pathways to neurodegeneration: effects of HIV and aging on resting-state functional connectivity. Neurology 80:1186–1193
30. Trebuchon A, Guye M, Tcherniack V, Tramoni E, Bruder N, Metellus P (2012) Interest of EEG recording during direct electrical stimulation for brain mapping function in surgery. Ann Fr Anesth Reanim 31:e87–e90
31. Wang L, Li K, Zhang QE, Zeng YW, Jin Z, Dai WJ, Su YA, Wang G, Tan YL, Yu X, Si TM (2013) Interhemispheric functional connectivity and its relationships with clinical characteristics in major depressive disorder: a resting state fMRI study. PLoS One 8:e60191
32. Wengenroth M, Blatow M, Guenther J, Akbar M, Tronnier VM, Stippich C (2011) Diagnostic benefits of presurgical fMRI in patients with brain tumours in the primary sensorimotor cortex. Eur Radiol 21:1517–1525
33. Xiong J, Parsons LM, Gao JH, Fox PT (1999) Interregional connectivity to primary motor cortex revealed using MRI resting state images. Hum Brain Mapp 8:151–156
34. Yang H, Chopp M, Weiland B, Zhang X, Tepley N, Jiang F, Schallert T (2007) Sensorimotor deficits associated with brain tumor progression and tumor-induced brain plasticity mechanisms. Exp Neurol 207:357–367
35. Yousry TA, Schmid UD, Alkadhi H, Schmidt D, Peraud A, Buettner A, Winkler P (1997) Localization of the motor hand area to a knob on the precentral gyrus. A new landmark Brain 120(Pt 1):141–157
36. Yu Y, Shen H, Zhang H, Zeng LL, Xue Z, Hu D (2013) Functional connectivity-based signatures of schizophrenia revealed by multiclass pattern analysis of resting-state fMRI from schizophrenic patients and their healthy siblings. Biomed Eng Online 12:10
37. Zeng H, Pizarro R, Nair VA, La C, Prabhakaran V (2013) Alterations in regional homogeneity of resting-state brain activity in mesial temporal lobe epilepsy. Epilepsia 54:658–666
38. Zhang D, Johnston JM, Fox MD, Leuthardt EC, Grubb RL, Chicoine MR, Smyth MD, Snyder AZ, Raichle ME, Shimony JS (2009) Preoperative sensorimotor mapping in brain tumor patients using spontaneous fluctuations in neuronal activity imaged with functional magnetic resonance imaging: initial experience. Neurosurgery 65: 226–236
39. Zhang LJ, Qi R, Zhong J, Ni L, Zheng G, Xu J, Lu GM (2013) Disrupted functional connectivity of the anterior cingulate cortex in cirrhotic patients without overt hepatic encephalopathy: a resting state fMRI study. PLoS One 8:e53206